environmental microbiology

Environmental Microbiology (2010) **12**(6), 1705–1718 doi:10.1111/j.1462-2920.2010.02245.x

The regulatory logic of *m*-xylene biodegradation by *Pseudomonas putida* mt-2 exposed by dynamic modelling of the principal node *Ps/Pr* of the TOL plasmid

Michalis Koutinas,[1†] Ming-Chi Lam,[1,2†] Alexandros Kiparissides,[1] Rafael Silva-Rocha,[3] Miguel Godinho,[2] Andrew G. Livingston,[1] Efstratios N. Pistikopoulos,[1] Victor de Lorenzo,[3] Vitor A. P. Martins dos Santos[2,4†] and Athanasios Mantalaris[1*†]**

[1]*Centre for Process Systems Engineering, Department of Chemical Engineering and Chemical Technology, South Kensington Campus, Imperial College London, London SW7 2AZ, UK.*

[2]*Systems and Synthetic Biology Group, Helmholtz Center for Infection Research (HZI), Inhoffenstrasse 7, D-38124 Braunschweig, Germany.*

[3]*Centro Nacional de Biotecnologia, Consejo Superior de Investigaciones Cientificas, Darwin 3, Cantoblanco, 28049 Madrid, Spain.*

[4]*Chair for Systems and Synthetic Biology, Wageningen University, Dreijenplein 310, 6703 HB Wageningen, the Netherlands.*

Summary

The structure of the extant transcriptional control network of the TOL plasmid pWW0 born by *Pseudomonas putida* mt-2 for biodegradation of *m*-xylene is far more complex than one would consider necessary from a mere engineering point of view. In order to penetrate the underlying logic of such a network, which controls a major environmental cleanup bioprocess, we have developed a dynamic model of the key regulatory node formed by the *Ps/Pr* promoters of pWW0, where the clustering of control elements is maximal. The model layout was validated with batch cultures estimating parameter values and its predictive capability was confirmed with independent sets of experimental data. The model revealed how regulatory outputs originated in the divergent and overlapping *Ps/Pr* segment, which expresses the transcription factors XylS and XylR respectively, are computed into distinct instructions to the *upper* and *lower* catabolic *xyl* operons for either simultaneous or stepwise consumption of *m*-xylene and/or succinate. In this respect, the model reveals that the architecture of the *Ps/Pr* is poised to discriminate the abundance of alternative and competing C sources, in particular *m*-xylene versus succinate. The proposed framework provides a first systemic understanding of the causality and connectivity of the regulatory elements that shape this exemplary regulatory network, facilitating the use of model analysis towards genetic circuit optimization.

Received 26 January, 2010; accepted 28 March, 2010. For correspondence. *E-mail a.mantalaris@imperial.ac.uk; Tel. (+44) 20 7594 5601; Fax: (+44) 20 7594 5638; **E-mail: vds@helmholtz-hzi.de; Tel. (+49) 531 6181 4008; Fax: (+49) 531 6181 4049. †These authors contributed equally to this work.

Introduction

Pseudomonas putida is a soil bacterium that is renowned for its metabolic versatility, thriving in diverse environments and competing successfully with other organisms (Pieper *et al.*, 2004). Several pseudomonads, including *P. putida* mt-2, have been reported to metabolize a large number of industrially important aromatics. This has led to a growing interest in studying these metabolic pathways at the gene expression and regulation levels (Ballerstedt *et al.*, 2007). The sequencing of *P. putida* strain KT2440 provided the means to investigate the metabolic potential of the *P. putida* species, and supported the development of new biotechnological processes (Wierckx *et al.*, 2008). Towards this end, large-scale mathematical models of the metabolism of *P. putida* have also been developed (Nogales *et al.*, 2008; Puchalka *et al.*, 2008) in an attempt to better understand the metabolism of this bacterium and to explore the vast biotechnological potential of this versatile microorganism.

Strain *P. putida* mt-2 is equipped with the TOL catabolic plasmid (pWW0), which specifies a pathway for the oxidative catabolism of toluene and *m*-xylene (Timmis, 2002). The enzymes required for these reactions are produced by the two gene operons of TOL (upper operon: *xyl*UWCMABN and *meta* operon: *xyl*XYZLTEGFJQKIH), while two genes (*xylS* and *xylR*) control the regulation of transcription of the gene operons (Fig. 1). These four transcriptional units are driven by four different promoters

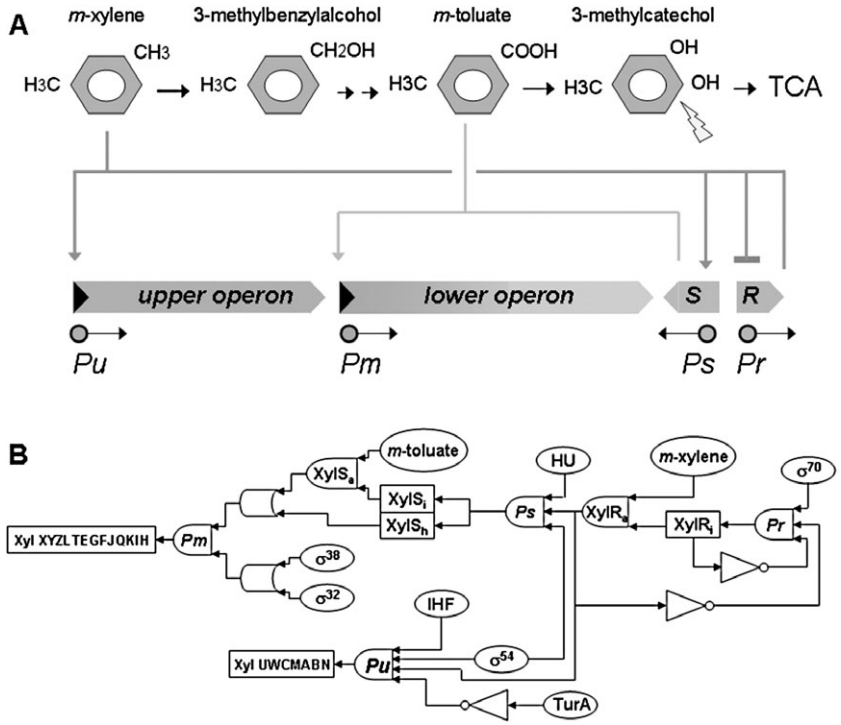

Fig. 1. Organization of the *m*-xylene biodegradation pathway born by the TOL plasmid pWW0. The figure sketches the reactions implicated in metabolism of this aromatic compound, including the stepwise oxidation of one methyl group of the substrate to an alcohol and eventually to a carboxylic acid, yielding *m*-toluate through the action of the enzymes encoded by the upper TOL pathway. *m*-toluate is then dioxygenated to yield 3-methylcatechol, which is cleaved in *meta* and finally channelled into the Krebs cycle by means of the products of the lower or *meta* operon. The upper operon is transcribed from the σ^{54} promoter *Pu* upon activation by the cognate regulator of the pathway (XylR) bound to specific effectors. These include the substrate of the pathway (*m*-xylene) as well as the two first metabolic intermediates: 3-methylbenzylalcohol and 3-methylbenzylaldehyde. The lower operon is transcribed from the *Pm* promoter, which is activated by the *m*-toluate responsive activator XylS. *Pm* can be turned on by either XylS and *m*-toluate as a co-inducer, or by overproduction of XylS alone. Finally, *xyl*S and *xyl*R are transcribed from the divergent and overlapping promoters *Ps* and *Pr* respectively. The regulation of the latter is connected, because the *Ps* promoter is activated by XylR, which also binds and downregulates its own *Pr* promoter. (A) TOL regulatory circuit, and (B) its logic implementation. TurA: TurA protein; $XylS_a$: active form of XylS; $XylS_i$: inactive form of XylS; $XylS_h$: hyperproduction of XylS; ⬭: input; ▭: output; ⊂: AND; ⊂(: OR; ▷: NOT.

(upper operon: *Pu*, *meta* operon: *Pm*, *xyl*S gene: *Ps* and *xyl*R gene: *Pr*). Due to the intricate interplay between plasmid-encoded and chromosome-encoding factors, the regulation of TOL operons is a paradigm of a prokaryotic gene expression circuit that processes numerous environmental and exogenous signals (Ramos *et al*., 1997). However, the regulatory network that controls expression of the catabolic operons appears in a first sight unnecessarily complex and somewhat burdensome. This raises the question of whether a functional explanation for such a complexity could be embodied in the circuit architecture but is beyond the standard, reductionist analysis of the singular regulatory components.

This work describes the development and validation of a dynamic mathematical model for a quantitative understanding of the complex control circuit of the TOL plasmid of *P. putida* mt-2. To this end, we concentrated in the region of the regulatory network that bears the highest regulatory density: the divergent *Ps/Pr* promoter region (Fig. 1). An initial map of the system was assembled integrating information about the interactions of the molecules involved into a representation, implementing logic gates. The dynamic model was constructed by combining the logic gate model with Hill functions, which have been extensively used to describe many real gene input functions (Alon, 2006). Initial estimates of model parameter values were obtained through a series of independent experiments, and the predictive capability of the model was evaluated in a carefully designed, distinct experimental set-up. Our results show that the dynamic model effectively describes the function of the system and its dynamics with a considerable accuracy. Furthermore, the architecture of the *Ps/Pr* node seems to mediate the ability of the system to discriminate between *m*-xylene and succinate as a preferred C source. This modelling framework provides a solid basis for a systemic understanding of the metabolism of representative environmental pollutants (i.e. xylenes) by *P. putida* strains. The dynamic model enables the use of model analysis tools for the formulation of genetic circuit optimization methods,

opening a window into the direct re-programming of cellular behaviour and, subsequently, the development of optimized and novel, high-added value biocatalysts.

Results and discussion

Rationale of the modelling frame

Genetic circuits are groups of elements that interact producing a certain behaviour (Weiss *et al*., 2003). The construction of the simple genetic circuits presented so far constitutes an initial attempt towards logical cellular control (Hasty *et al*., 2002). Based on our capability to simulate genetic circuits, fundamental biological processes can be studied systematically and targets can be identified for genetic modification at the DNA level, producing a desired behaviour. However, the extensive experimentation required to understand the function of genetic circuits is often limited by the time or cost required. Moreover, experiments are usually designed on a trial and error basis and the information gained, although vast, is scattered. The use of a systematic framework for the design of optimally informative experiments through model-based techniques can significantly reduce unnecessary experimentation and cost (Kontoravdi *et al*., 2005). Furthermore, model analysis techniques, such as global sensitivity analysis (GSA), can provide behavioural information regarding the hierarchical structure of the modelled system that would otherwise be hard to extract from experimental observations alone (Kiparissides *et al*., 2009).

The level of detail incorporated in a mathematical description of a system is a function of the available biological information on the said system, the availability and feasibility of experimental measurements for the majority of the variables involved and the scope of the model (De Jong, 2002). Different model-based methodologies can be established in order to elucidate the properties of biological systems such as: (i) design and modification, (ii) structure, (iii) dynamics, and (iv) control methods (Kitano, 2001). Dynamic modelling can be used for the characterization of the physiological behaviour of cells integrating biological information into predictive models (Sidoli *et al*., 2004). The translation of the logic inherent in a genetic circuit representation into dynamic models embedded in a holistic experimental and modelling framework proposes a novel future direction linking the function of genetic circuits to cellular and consequently to bioprocess behaviour.

Mathematical modelling of the Ps/Pr *promoters system*

The mathematical model described here attempts to formalize the molecular mechanisms that control the functioning of the divergent *Ps/Pr* promoters of the TOL plasmid for *m*-xylene metabolism. The function of the genetic circuit used for model development (Fig. 1A) is based on existing biological knowledge (Ramos *et al*., 1997; Aranda-Olmedo *et al*., 2006) and observed mt-2 culture behaviour during the experiments. This is defined here globally by the genes, their products and molecules used on the catabolism of *m*-xylene. This definition does not take into account the function of the two TOL operons or the function encoded in its 116 kb genome for transposition, plasmid replication or other functions (Greated *et al*., 2002), since only the respective regulatory genes have been used for the construction of the genetic circuit. The system has been reconstructed into its various interacting molecular components and has been conceptually described as a combination of logic gates (Fig. 1B), based on biochemical inverters (Weiss, 2001). Consequently, an 'electronic' representation of the system has been obtained following an analogy to electronic circuitry. Therefore, by combining logic gates with each other results in the production of a simple description of the various regulatory loops and their expression. Based on the logic model of the *Ps/Pr* system (Fig. 2), Hill functions were used as input functions to the genes (Rosenfeld *et al*., 2005) and a dynamic mathematical model of the system was generated, as described below.

Pseudomonas putida mt-2 degrades aromatic substrates, such as toluene and xylenes, through a series of events leading to coordinated expression from the upper- and *meta*-cleavage pathways coded by the TOL plasmid. The master regulator of the two pathways, the XylR protein, is the product of the transcription of the *xylR* gene from two σ^{70} tandem promoters (*Pr1* and *Pr2*). After binding with *m*-xylene, the inactive dimer form of the XylR protein ($XylR_i$) binds ATP and oligomerizes to form a hexamer, which undergoes conformational changes (Bertoni *et al*., 1998). This effect leads to the formation of the active, from a transcriptional point of view, form of XylR ($XylR_a$), which induces transcription of the *Pu* promoter triggering the synthesis of the upper-pathway enzymes. The synthesis of $XylR_i$ from *Pr*, as well as the forward and reverse reactions of the mechanism for XylR activation/deactivation are expressed by Eqs 1 and 2:

$$\frac{dXylR_i}{dt} = \frac{\beta_{XylR_i} Pr_{TC}}{K_{Pr,XylR_i} + Pr_{TC}} - r_{XylR} XylR_i Xyl + 3r_{R,XylR} XylR_a (Xyl_{INI} - Xyl) - \alpha_{XylR_i} XylR_i \quad (1)$$

$$\frac{dXylR_a}{dt} = \frac{1}{3} r_{XylR} XylR_i Xyl - r_{R,XylR} XylR_a (Xyl_{INI} - Xyl) - \alpha_{XylR_a} XylR_a \quad (2)$$

where $XylR_i$ and $XylR_a$ refer to the concentrations of the inactive and active forms of XylR protein, respectively, r_{XylR} is the $XylR_i$ oligomerization constant, $r_{R,XylR}$ is the $XylR_a$ dissociation constant, Xyl is the total *m*-xylene concentration, Xyl_{INI} is the total *m*-xylene initial concentration, *t* is the time, Pr_{TC} is the relative activity of *Pr*, β_{XylRi} is the maximal

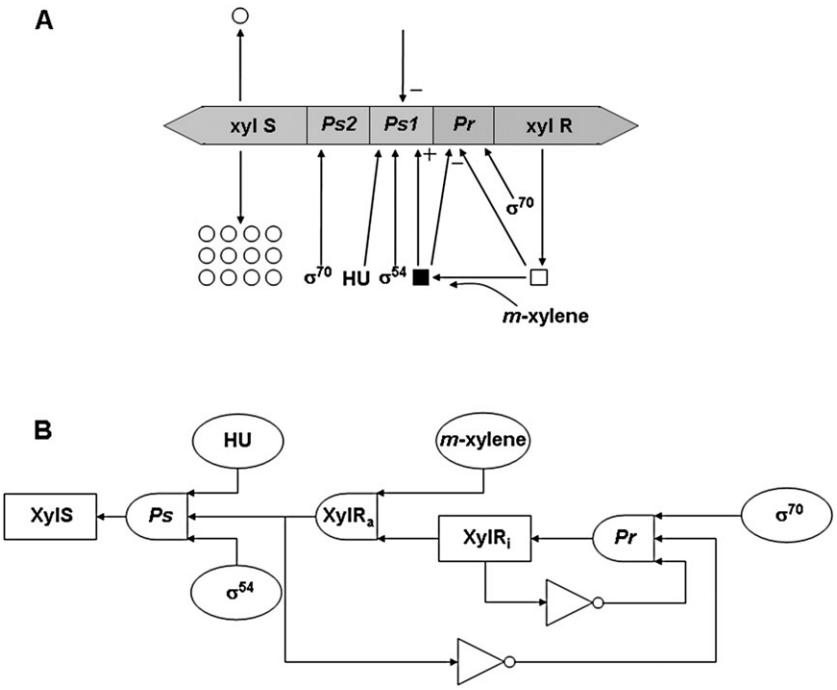

Fig. 2. A simplified view of the *Ps/Pr* system of TOL plasmid pWW0 encoded by *P. putida* mt-2. (A) The regulatory circuit controlling the expression from the *Ps/Pr* promoters of the TOL plasmid (adapted from Ramos *et al*., 1997), and (B) its logic implementation. □: $XylR_i$; ■: $XylR_a$; ○: XylS (inactive); +: stimulation of transcription; –: inhibition of transcription; ⬭: input; ▭: output; ⊂: AND; ▷: NOT.

$XylR_i$ translation rate based on *Pr* activity, $K_{Pr,XylRi}$ is the $XylR_i$ translation coefficient and α_{XylRi} and α_{XylRa} account for degradation and dilution due to cellular volume increase for $XylR_i$ and $XylR_a$ respectively.

For simplification of the model developed we express both *xylR* tandem promoters as a single *Pr* promoter. The XylR binding sites activating *Ps* overlap with the σ^{70} activated *Pr* promoter, repressing its expression and thus its own synthesis. Expression from *Pr* is repressed when either $XylR_i$ or $XylR_a$ bind to the UASs of *Pr* (Marques *et al*., 1998). Furthermore, it has been previously shown that σ^{70} concentration in *Escherichia coli* is high in all growth phases (Ishihama, 2000). Consequently, we assumed that the concentration of σ^{70} is constant at housekeeping level. During the parameter estimation experiments presented below, the *Pr* promoter was slightly repressed when both succinate and *m*-xylene were fed as compared with the case when the culture was exposed only to *m*-xylene. Therefore, we assumed that succinate is repressive for *Pr* promoter expression in the presence of *m*-xylene and thus in Eq. 3, describing the activity of *Pr* promoter, $K_{SUC,Pr} = 0\ mM^{-2}$ when only succinate is fed.

$$\frac{dPr_{TC}}{dt} = \frac{\beta_{Pr}}{1+\left(\frac{XylR_i}{K_{XylR_i}}\right)^{n_{Pr,i}}+\left(\frac{XylR_a}{K_{XylR_a}}\right)^{n_{Pr,a}}} \frac{1}{1+K_{SUC,Pr}Suc^2} - \alpha_{Pr}Pr_{TC} \quad (3)$$

β_{Pr} stands for the maximal expression level of *Pr*, K_{XylRi} and K_{XylRa} are the repression coefficients of *Pr* due to $XylR_i$ and $XylR_a$ binding, respectively, $n_{Pr,i}$ and $n_{Pr,a}$ are the Hill coefficients of *Pr* due to $XylR_i$ and $XylR_a$ binding, respectively, *Suc* is succinate concentration, $K_{SUC,Pr}$ is the inhibition constant of succinate on *Pr* activity, and α_{Pr} is the deactivation rate of *Pr*.

The *xylS* gene is expressed constitutively at low levels but boosted in the presence of *m*-xylene. One explanation is that *xylS* is transcribed from *Ps1* and *Ps2* promoters. Transcription from the σ^{54} dependent *Ps1* promoter is induced when *m*-xylene is present, whereas transcription from the σ^{70}-dependent *Ps2* promoter is low and constitutive (Gonzalez-Perez *et al*., 2004). Therefore, in the presence of *m*-xylene *Ps2* remains constant at low levels, whereas *Ps1* is induced by $XylR_a$. An alternative model claims that only one σ^{54} promoter *Ps* transcribes *xylS*, but the gene is expressed constitutively in the absence of *m*-xylene owing to the cross-regulation by other enhancer-binding proteins (Perez-Martin and de Lorenzo, 1995). For the sake of this work and regardless of the specific mechanism, we name as *Ps1* the promoter activity that is triggered exclusively by $XylR_a$, while we designate *Ps2* as the source of transcription that is independent of $XylR_a$ and is always active at a basal expression level β_0 (Eq. 4). The combined function of *Ps1* and *Ps2* promoters is referred in the rest of the manuscript as the *Ps* promoter. In cells growing with a XylS effector (e.g. benzoate), XylS binds the effector and stimulates transcription from *Pm* (*meta*-pathway promoter). However, in cells growing on *m*-xylene, the high XylS concentration synthesized is sufficient to stimulate transcription from *Pm* and allow the coordinate induction of the two pathways (Ramos *et al*., 1987).

Activation of *Ps* is assisted by the HU protein, which binds and bends *Ps* DNA bringing the UAS and the σ^{54}-RNAP together, thus stabilizing the correct architecture of the promoter (Perez-Martin and de Lorenzo, 1995). It has been previously reported that the σ^{54}-dependent promoters *Pu* and *Ps* are directly or indirectly negatively affected in the presence of repressive carbon sources, such as succinate or glucose (Duetz *et al*., 1994; Holtel *et al*., 1994). This has been also confirmed in the parameter estimation experiments of this study and we therefore consider that succinate is repressive for *Ps* promoter expression. Furthermore, we assume that the concentration of HU and σ^{54} is constant at housekeeping level. Based on previous findings, HU is abundant in *E. coli* (Ishihama, 1999). Furthermore, σ^{54} is a constitutive protein (Merrick, 1993) maintaining the same intracellular concentration throughout the growth time (Cases *et al*., 1996; Jishage *et al*., 1996). Although there is evidence that competition takes place between the σ subunits for binding the core enzyme and that the number of σ^{54} molecules per cell in *P. putida* is barely above the number of σ^{54}-dependent promoters (Jurado *et al*., 2003), due to the lack of experimental information about σ^{54} concentration, it is assumed that σ^{54} is not limiting.

There are conflicting reports in the literature regarding the function of IHF protein as a negative regulator of *Ps* promoter expression. Although previous studies support that IHF significantly represses *Ps* promoter activity *in vivo* (Holtel *et al*., 1995; Marques *et al*., 1998), based on our own research we advocate that IHF binding at *Ps* is quite weak and its effect is basically negligible. The repressor effect in question is present only at high IHF concentrations (de Lorenzo *et al*., 1991), while under inducing conditions $XylR_a$ binds strongly to *Ps*, which it is not significantly affected by IHF (Holtel *et al*., 1992). Since IHF competes weakly for a part of the sequence under induced conditions, we have assumed the function of *Ps* as IHF-independent. *Ps* promoter activity is given by Eq. 4.

$$\frac{dPs_{TC}}{dt} = \beta_0 + \beta_{Ps}\frac{XylR_a^{n_{Ps,a}}}{K_{XylR_a,Ps}^{n_{Ps,a}} + XylR_a^{n_{Ps,a}}}\frac{1}{1+\left(\frac{Suc}{K_{SUC,Ps}}\right)^2} - \alpha_{Ps}Ps_{TC} \quad (4)$$

Ps_{TC} stands for the relative activity of *Ps*, β_0 is the basal expression level of *Ps*, β_{Ps} is the maximal expression level of *Ps*, $K_{XylRa,Ps}$ is the activation coefficient of *Ps*, $n_{Ps,a}$ is the Hill coefficient of *Ps*, $K_{SUC,Ps}$ is the inhibition constant of succinate on *Ps* activity and α_{Ps} is the deactivation rate of *Ps*.

Although it has been previously shown that gene expression information both at the message and the protein level is required to describe even simple models of genetic circuits (McAdams and Shapiro, 1995; Hatzimanikatis and Lee, 1999), the present mathematical model does not account for the dynamics of mRNA transcription from *Pr*. This approach was followed to avoid the introduction of a significant number of parameters and state variables for which dynamic measurements were not feasible, thus resulting in a more detailed set of equations but with highly correlated parameters. A more complete mechanistic understanding of the system could have been given with the use of mass action kinetics and elementary reactions instead of the use of Hill functions (Radivoyevitch, 2009). However, the reaction scheme of the system in the present study is very complex and thus it would lead in a large model with many parameters to be estimated. Consequently, the lumped, yet still biologically relevant, 3-parameter Hill model was chosen. The K parameter is termed activation or repression coefficient, depending on whether the transcription factor acts as activator or repressor, and defines the concentration of the transcription factor required to significantly activate or repress expression. The second parameter (β) is the maximal expression level of the promoter, which is reached at high activator concentrations, while the third parameter *n* is the Hill coefficient determining the steepness of the input function. Furthermore, the model does not describe cell growth or the consumption of the two substrates. Therefore, *m*-xylene and succinate concentrations are given from best-fit time profiles of their experimental values (Fig. 3A–D). The model presented above was implemented in gPROMS (Process Systems Enterprise, 1997–2010) and the parameter values, given in Tables 1 and 2, were obtained from three batch experiments with different combinations of carbon sources.

Parameter estimation experiment I: succinate only

We first studied the performance of the system in the absence of TOL pathway effectors, supplying the culture with 13.6 mM succinate as the sole carbon source. According to the logic model presented in Fig. 2B, when *m*-xylene is not present, $XylR_a$ is not produced. Consequently, *Ps* was expected to be silent and *Pr* should be repressed as a result of the $XylR_i$ synthesized. The expected system behaviour was confirmed by the experimentally obtained relative activity profiles of the two promoters, as shown in Fig. 4A and B. One model parameter value (β_0) was estimated from the experimental relative activity of *Ps*, while seven parameter values ($K_{Pr,XylRi}$, K_{XylRi}, $n_{Pr,i}$, α_{Pr}, α_{XylRi}, β_{Pr} and β_{XylRi}) were estimated from the experimental relative activity of *Pr*.

Parameter estimation experiment II: m-xylene only

In order to study the behaviour of the system in the presence of a TOL pathway effector, the second parameter

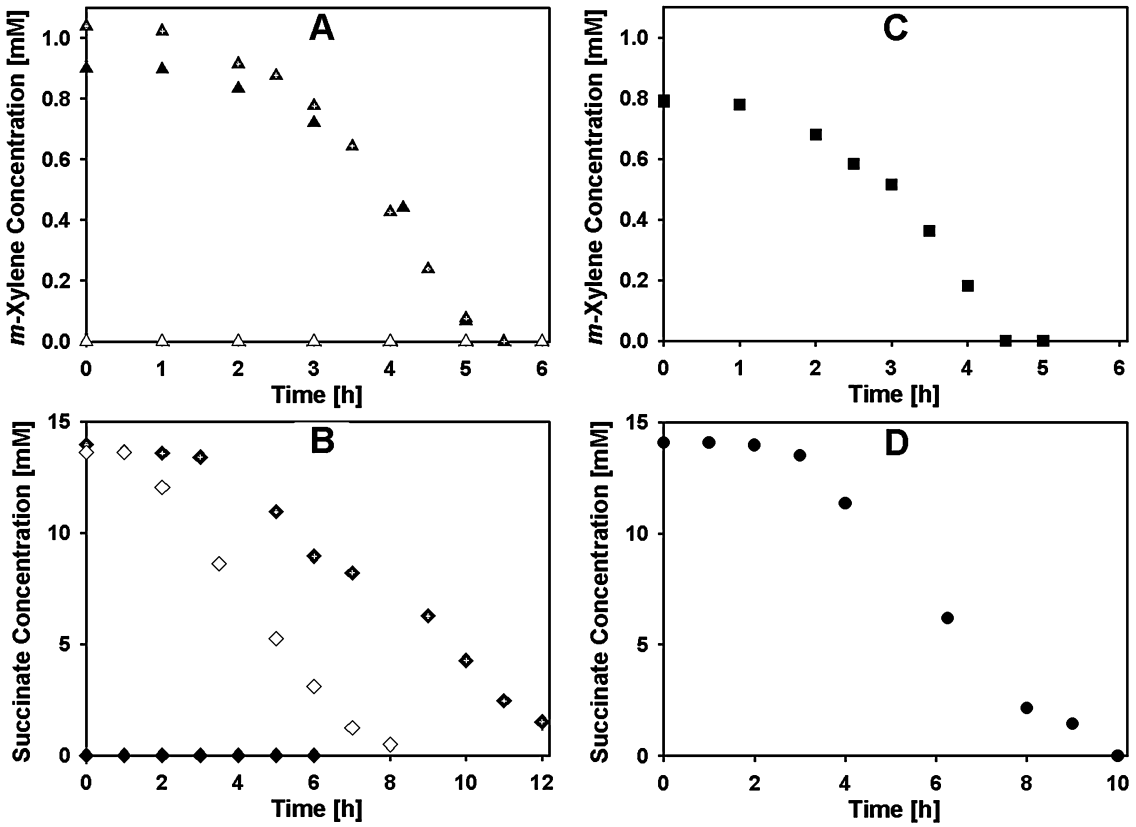

Fig. 3. Concentrations of the two substrates in the experiments. (A) *m*-Xylene concentration (parameter estimation experiments), (B) succinate concentration (parameter estimation experiments), (C) *m*-xylene concentration (predictive experiment), and (D) succinate concentration (predictive experiment). ▲: *m*-xylene concentration – *m*-xylene only; △: *m*-xylene concentration – succinate only; ◬: *m*-xylene concentration – succinate and *m*-xylene; ◆: succinate concentration – *m*-xylene only; ◇: succinate concentration – succinate only; ❖: succinate concentration – succinate and *m*-xylene; ■: *m*-xylene concentration – predictive experiment; ●: succinate concentration – predictive experiment.

estimation experiment was conducted in the presence of 0.9 mM *m*-xylene as the sole carbon source. Under induced conditions, $XylR_i$ is oligomerized to form $XylR_a$ and *Ps* promoter is activated increasing its relative activity (Fig. 4B). The increase in *Ps* activity was confirmed by statistical analysis showing that *Ps* expression at 2 h and 3 h was significantly different ($P < 0.05$) when compared with the initial time points (0, 0.17 and 1 h). When *m*-xylene was exhausted *Ps* activity was expected to decrease to its basal level. However, the *Ps* promoter's relative activity was maintained at significantly higher level than its basal activity for at least 5 h following the onset of the stationary phase (data not shown). Although the activation of σ^{54} promoters in stationary phase has been previously described (Cases *et al*., 1996), the prediction of the system's performance at stationary phase is out of the scope of the present study and has not been included in the model.

The *Pr* promoter was repressed (Fig. 4A) due to the presence of the two forms of its protein product ($XylR_i$, $XylR_a$). The repressory effect of $XylR_a$ was removed, due to an expected $XylR_a$ concentration decrease when *m*-xylene was exhausted. Thus, the relative activity of the *Pr* promoter increased at the beginning of the stationary phase (5 h) to a significantly higher level compared with all previous time points. The *m*-xylene concentrations of the three triplicate cultures used for the experiment at 5 h were 0, 0.07 and 0.13 mM respectively. The large standard deviation of the *Pr* promoter's relative activity value at 5 h was due to the fact that the promoter's activity for the two cultures with lower *m*-xylene concentration was higher than 4.50 (dimensionless), while that of the culture with higher *m*-xylene concentration was 0.27 (dimensionless). This, most likely, represents an indication for a fast dissociation of $XylR_a$ forming $XylR_i$, when *m*-xylene concentration is completely exhausted leading to a rapid increase of *Pr* promoter activity. As shown in Tables 1 and 2, five model parameter values (K_{XylRa}, $n_{Pr,a}$, $r_{R,XylR}$ and α_{XylRa}) were estimated from the experimentally determined relative activity of *Pr* and four parameter values (α_{Ps}, $K_{XylRa,Ps}$, $n_{Ps,a}$ and β_{Ps}) were estimated from the relative activity of *Ps*.

Table 1. Parameter values related to *Pr* promoter used for model simulation.

Parameter	Equation used	Simplified equation	Value	Experiment obtained
K_{XylRi}	3	$\frac{dPr_{TC}}{dt} = \frac{\beta_{Pr}}{1+\left(\frac{XylR_i}{K_{XylR_i}}\right)^{n_{Pr,i}}} - \alpha_{Pr}Pr_{TC}$	1.225 mM	Succinate only
$K_{Pr,XylRi}$	1	$\frac{dXylR_i}{dt} = \frac{\beta_{XylR_i}Pr_{TC}}{K_{Pr,XylR_i}+Pr_{TC}} - \alpha_{XylR_i}XylR_i$	2.133 [–]	Succinate only
$n_{Pr,i}$	3	$\frac{dPr_{TC}}{dt} = \frac{\beta_{Pr}}{1+\left(\frac{XylR_i}{K_{XylR_i}}\right)^{n_{Pr,i}}} - \alpha_{Pr}Pr_{TC}$	2 [–]	Succinate only
α_{Pr}	3	$\frac{dPr_{TC}}{dt} = \frac{\beta_{Pr}}{1+\left(\frac{XylR_i}{K_{XylR_i}}\right)^{n_{Pr,i}}} - \alpha_{Pr}Pr_{TC}$	3.157 h^{-1}	Succinate only
α_{XylRi}	1	$\frac{dXylR_i}{dt} = \frac{\beta_{XylR_i}Pr_{TC}}{K_{Pr,XylR_i}+Pr_{TC}} - \alpha_{XylR_i}XylR_i$	2.132 h^{-1}	Succinate only
β_{Pr}	3	$\frac{dPr_{TC}}{dt} = \frac{\beta_{Pr}}{1+\left(\frac{XylR_i}{K_{XylR_i}}\right)^{n_{Pr,i}}} - \alpha_{Pr}Pr_{TC}$	7.209 h^{-1}	Succinate only
β_{XylRi}	1	$\frac{dXylR_i}{dt} = \frac{\beta_{XylR_i}Pr_{TC}}{K_{Pr,XylR_i}+Pr_{TC}} - \alpha_{XylR_i}XylR_i$	5.728 mM h^{-1}	Succinate only
K_{XylRa}	3	$\frac{dPr_{TC}}{dt} = \frac{\beta_{Pr}}{1+\left(\frac{XylR_i}{K_{XylR_i}}\right)^{n_{Pr,i}}+\left(\frac{XylR_a}{K_{XylR_a}}\right)^{n_{Pr,a}}} - \alpha_{Pr}Pr_{TC}$	0.04179 mM	*m*-Xylene only
$n_{Pr,a}$	3	$\frac{dPr_{TC}}{dt} = \frac{\beta_{Pr}}{1+\left(\frac{XylR_i}{K_{XylR_i}}\right)^{n_{Pr,i}}+\left(\frac{XylR_a}{K_{XylR_a}}\right)^{n_{Pr,a}}} - \alpha_{Pr}Pr_{TC}$	2 [–]	*m*-Xylene only
$r_{R,.XylR}$	1	Not simplified	7.806 mM^{-1} h^{-1}	*m*-Xylene only
r_{XylR}	1	Not simplified	2.589 mM^{-1} h^{-1}	*m*-Xylene only
α_{XylRa}	2	Not simplified	2.716 h^{-1}	*m*-Xylene only
$K_{SUC,Pr}$	3	Not simplified	1.029 mM^{-2}	Succinate and *m*-xylene

Parameter estimation experiment III: succinate and m-xylene

In order to test the behaviour of the system under the presence of a combination of the two differential carbon sources, a batch culture was performed with 1.04 mM *m*-xylene and 14 mM succinate. As expected, the *Ps* promoter was repressed in the presence of succinate due to catabolite repression (Ramos *et al.*, 1997) and its activity reached a lower maximum compared with the *m*-xylene only cultures (Fig. 4B). Similar behaviour was also observed for the *Pr* promoter, which was repressed in the presence of both substrates as compared with when only *m*-xylene was fed (Fig. 4A). Interestingly, the activity of the *Pr* promoter did not increase when *m*-xylene was exhausted. This probably indicates that the inhibition of the *Pr* promoter in the presence of both carbon sources may have a different mechanism as compared with when only *m*-xylene is present. For this reason, an inhibitory term was introduced to the model when both substrates are present, although such behaviour has never been reported before. The inhibition constants of succinate on *Pr* and *Ps* promoters activities ($K_{SUC,Pr}$ and $K_{SUC,Ps}$ respectively) were estimated from the experimentally determined relative activities of the two promoters in the double substrate experiment.

Predictive experiment

To demonstrate the model's predictive capability, model simulation results were compared with an independent set of data. The initial succinate concentration was the same as in the parameter estimation experiments

Table 2. Parameter values related to *Ps* promoter used for model simulation.

Parameter	Equation used	Simplified equation	Value	Experiment obtained
α_{Ps}	4	$\frac{dPs_{TC}}{dt} = \beta_0 - \alpha_{Ps}Ps_{TC}$	0.665 h^{-1}	*m*-Xylene only
β_0	4	$\frac{dPs_{TC}}{dt} = \beta_0 - \alpha_{Ps}Ps_{TC}$	7.459×10^{-3} h^{-1}	Succinate only
$K_{XylRa,Ps}$	4	$\frac{dPs_{TC}}{dt} = \beta_0 + \beta_{Ps}\frac{XylR_a^{n_{Ps,a}}}{K_{XylR_a,Ps}^{n_{Ps,a}} + XylR_a^{n_{Ps,a}}} - \alpha_{Ps}Ps_{TC}$	1.419×10^{-6} mM	*m*-Xylene only
$n_{Ps,a}$	4	$\frac{dPs_{TC}}{dt} = \beta_0 + \beta_{Ps}\frac{XylR_a^{n_{Ps,a}}}{K_{XylR_a,Ps}^{n_{Ps,a}} + XylR_a^{n_{Ps,a}}} - \alpha_{Ps}Ps_{TC}$	5 [–]	*m*-Xylene only
β_{Ps}	4	$\frac{dPs_{TC}}{dt} = \beta_0 + \beta_{Ps}\frac{XylR_a^{n_{Ps,a}}}{K_{XylR_a,Ps}^{n_{Ps,a}} + XylR_a^{n_{Ps,a}}} - \alpha_{Ps}Ps_{TC}$	2.319 h^{-1}	*m*-Xylene only
$K_{SUC,Ps}$	4	Not simplified	9.307 mM	Succinate and *m*-xylene

(14.1 mM), while *m*-xylene concentration was reduced to 0.8 mM. This decrease in *m*-xylene concentration by 23%, as compared with the parameter estimation experiment III, is far from negligible considering the toxic nature of the compound as the same increment, were it an increase instead of a decrease, might have been fatal for the culture. Furthermore, as depicted in Fig. 4B, in the absence of an effector of the TOL pathway *Ps* promoter remains inactive, a response that is also expected for the promoters controlling the transcription of the upper- and meta-pathway operons. Thus, the effect of the aromatic compound on the TOL plasmid gene network is more pronounced both from a biological and modelling point of view and the concentration of succinate should not directly affect the behaviour of the promoters. Due to this rationale we conclude that *m*-xylene concentration strongly affects the behaviour of TOL and for this reason we did not consider necessary varying the concentration of succinate. The overall trend of the model prediction for the *Pr* promoter relative activity is accurate, as confirmed by correlating the model's prediction with 95% confidence intervals of *Pr* activity, tracking the experimental results satisfactorily (Fig. 5A). Similarly, the model's prediction closely tracks the relative activity of *Ps* for the first 3 h of the culture, with some discrepancies between 3 and 5 h when *Ps* activity is somewhat overpredicted (Fig. 5B), as confirmed by 95% confidence intervals of the experimental data. The results of the predictive experiment validate that the existing model structure can effectively describe the experimental data of the relative activity of the two promoters based on the level of biological information available for the system.

XylR$_i$ and XylR$_a$ concentration profiles

The concentration profile of the master regulator of TOL (XylR) in the two forms it assumes (XylR$_i$ and XylR$_a$) is critical for the accurate prediction of the behaviour of the system. The predicted concentration profiles of XylR$_i$ and XylR$_a$, according to the mechanism described by Eqs 1 and 2, is shown in Fig. 6. Because the concentrations of XylR$_i$ and XylR$_a$ were not measured, we considered the case where both proteins were initially absent and their production starts at the beginning of the culture.

At the start of the succinate-only culture, when the XylR$_i$ concentration is still low, *Pr* is unrepressed and XylR$_i$ production is constant at the rate β_{XylRi} (Fig. 6A), taking into account that XylR$_a$ is not produced in the absence of *m*-xylene. In fact, early on, XylR$_i$ degradation can be ignored, resulting in almost linear accumulation of the protein over time. As XylR$_i$ concentration increases beyond a self-repression threshold value, its production slows down. A small oscillation observed in *Pr* activity (Fig. 4A) is, as expected, apparent in the production of XylR$_i$, a fact that occurs when delays occur in the system (Alon, 2006). Therefore, such delays may be responsible for the overshoot in XylR$_i$ concentration, which eventually decreases to a steady-state level for the remaining of the culture.

In the *m*-xylene only cultures, XylR$_i$ concentration initially increases reaching a lower maximum due to the oligomerization of the protein forming XylR$_a$ (Fig. 6B). However, when the *m*-xylene concentration decreases, XylR$_a$ concentration also declines forming XylR$_i$, which leads to increased levels of XylR$_i$ concentration. As shown previously, when both carbon sources are present *Pr* activity is repressed. Thus, expression from *Pr* is lower leading to lower XylR$_i$ and XylR$_a$ concentrations.

Structural analysis of TOL

Expression of the *Pr* promoter is high regardless of the growth phase (Ramos *et al*., 1997). In the TOL plasmid, a negatively auto-regaled strong promoter (*Pr*) is used for

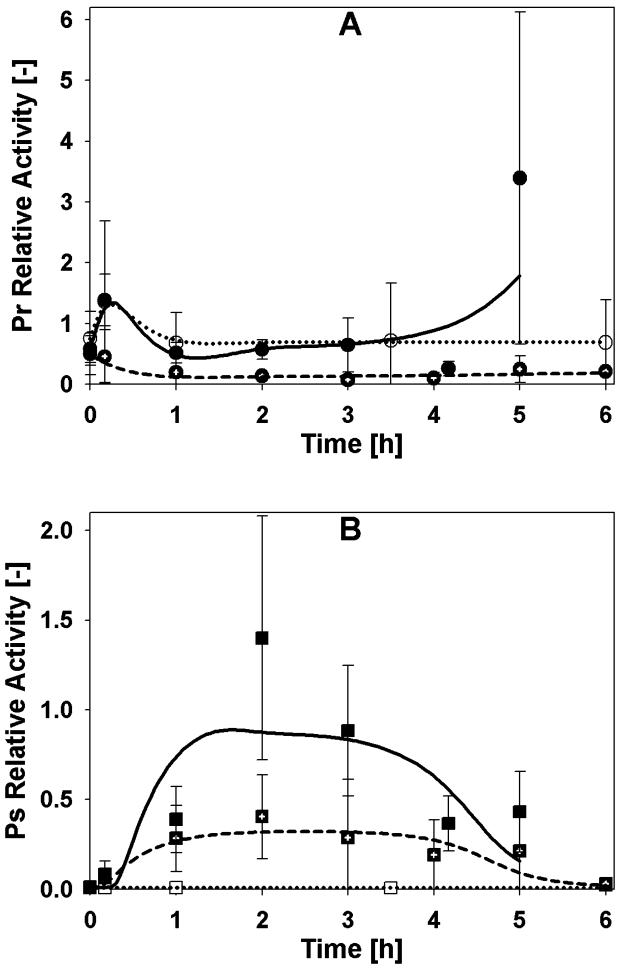

Fig. 4. *Pr* and *Ps* promoters' relative activity in parameter estimation experiments. (A) *Pr* promoter activity and (B) *Ps* promoter activity. ●: *m*-xylene only (*Pr* activity – experimental); ○: succinate only (*Pr* activity – experimental); ⊙: succinate and *m*-xylene (*Pr* activity – experimental); ■: *m*-xylene only (*Ps* activity – experimental); □: succinate only (*Ps* activity – experimental); ◘: succinate and *m*-xylene (*Ps* activity – experimental); ——: *m*-xylene only (*Pr* and *Ps* activity – predicted); ·····: succinate only (*Pr* and *Ps* activity – predicted); – – –: succinate and *m*-xylene (*Pr* and *Ps* activity – predicted).

the rapid production of the protein required to control expression from its catabolic operons and for the rapid balance of its production at a steady state. In addition to accelerating the response time of XylR production, the negative autoregulation of *Pr* might also provide a mechanism for homogeneously distributing its protein product within optimal concentration limits (Becskei and Serrano, 2000). Thus, the double negative autoregulation of *Pr* by $XylR_i$ and $XylR_a$ might buffer fluctuations in XylR production rate in the presence or absence of effectors, thus promoting robustness of the steady-state expression level of the master regulator of TOL.

For the given conditions in the present study, the simplification that production of IHF and HU proteins, which are necessary for activation of *Pu* and *Ps* promoters respectively, does not change over culture time can be made. Therefore, transcription from *xyl*UWCMABN (upper operon) and *xylS* is dependent only on the presence of the master regulator. The behaviour of such a system constitutes a single-input module (SIM), which is a network motif previously described (Shen-Orr *et al.*, 2002). SIMs usually regulate genes of a specific metabolic pathway and can generate temporal programs of expression, where the genes of a pathway are expressed in a defined order (Zaslaver *et al.*, 2004). The autogenous control of the master regulator of TOL is a common feature of SIMs where the master regulator is often autorepressed to optimally respond to multiple levels of input signal, thus minimizing the energetic cost of the cell's response to the presence of a pollutant (Camas *et al.*, 2006).

Expression of the *meta*-pathway in the presence of *m*-xylene is under the control of a two-stage cascade,

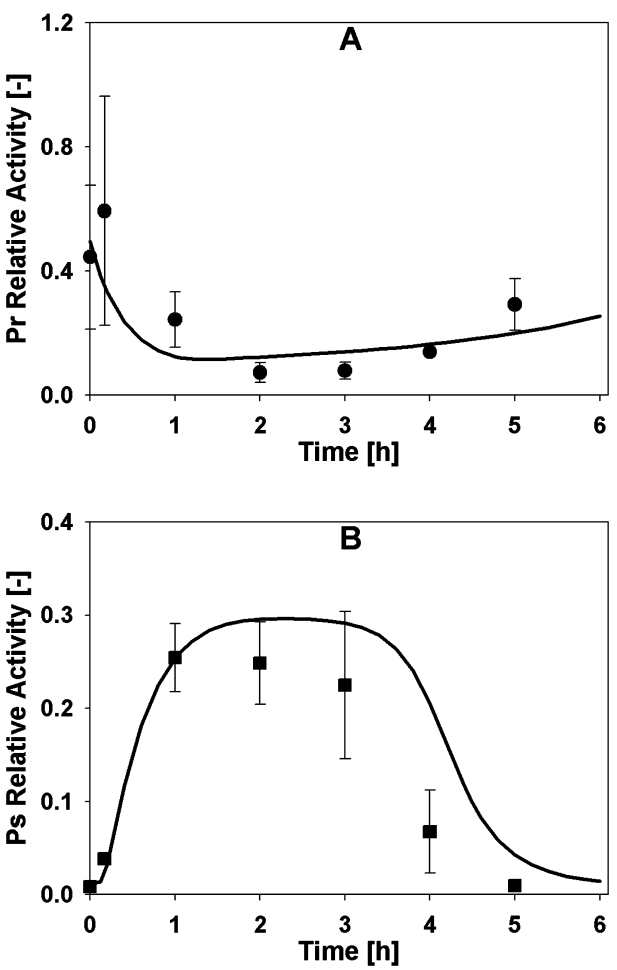

Fig. 5. *Pr* and *Ps* promoters' relative activity in the predictive experiment. (A) *Pr* promoter activity and (B) *Ps* promoter activity. ●: *Pr* activity – experimental; ■: *Ps* activity – experimental; ——: *Pr* and *Ps* activity – predicted.

constituting of *xylS* expression due to $XylR_a$ activation and expression of the genes of the *meta* operon (*xylX*-YZLTEGFJQKIH) driven by XylS binding. Cascades direct temporal programs of gene expression and are often met within complex networks including additional control mechanisms, such as SIMs (Hooshangi *et al.*, 2005). This is also the case in the TOL system, where a cascade of genes controls expression from the *meta* operon, being a part of the SIM activated in the presence of *m*-xylene.

The establishment of programmable biocatalysts performing efficiently specific biotechnological functions will require the optimization of genetic circuits of interest. Although the dynamics of genetic circuits is inherently oversimplified with the use of Boolean models, a more comprehensive description can be obtained with the use of dynamic models allowing the use of analytical techniques of non-linear dynamics. The complex coupling of the two catabolic pathways encoded in TOL with the multitude of interactions between the various regulatory molecules makes this system an example of the complexity that naturally occurring genetic circuits may incorporate. The mathematical model presented in this study furthers our understanding of the dynamic properties of this biological system and can set the basis for the development of a dynamic model for the whole TOL network (including predictions of expression from the catabolic operons). Consequently, the combination of the constructed model with model analysis techniques can device a model-based methodology identifying the driving mechanisms of the system, which can be used for hypothesis testing and network optimization. In the future, research will be aimed at understanding the evolution of the extant TOL network topology and dynamics in contrast with other possible forward-designed regulatory architectures.

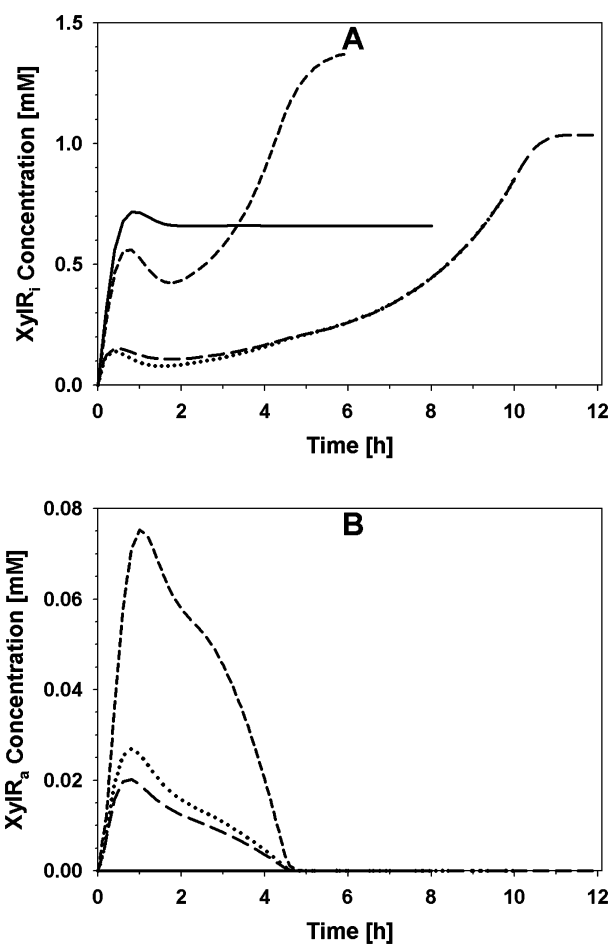

Fig. 6. Theoretical prediction of $XylR_i$ and $XylR_a$ concentrations. (A) $XylR_i$ concentration and (B) $XylR_a$ concentration. ——: Succinate only ($XylR_i$ or $XylR_a$ concentrations – predicted); - - -: *m*-Xylene only ($XylR_i$ or $XylR_a$ concentrations – predicted); ·····: Succinate and *m*-xylene ($XylR_i$ or $XylR_a$ concentrations – predicted); — —: Predictive experiment ($XylR_i$ or $XylR_a$ concentrations – predicted).

Experimental procedures

Microorganism and growing conditions

Subcultures of *P. putida* mt-2 were pre-grown overnight at 30°C in M9 minimal medium (Sambrook *et al.*, 1989) supplemented with 15 mM succinate as a carbon source. Triplicate cultures were prepared by diluting the overnight culture in minimal medium to an initial optical density of 0.1 at 600 nm. The minimal medium was supplemented either with succinate, *m*-xylene or a combination of the two carbon sources, at a concentration level in agreement to the requirements of each experiment. The incubation of the cultures was performed using conical flasks with 2.35 l total volume (0.4 l culture volume), which were continuously stirred at 1250 r.p.m. via a Heidolph MR 3001 K (Heidolph, UK) magnetic stirrer. Temperature was maintained constant at 30°C. All chemicals used were obtained from Sigma-Aldrich Company (UK) and were of ANALAR grade. *m*-Xylene was obtained from VWR International (UK) 99% pure.

Analyses

Gas chromatograph (GC) analysis was used for determination of the *m*-xylene concentration in the gaseous and aqueous samples. An Agilent 6850 Series II GC with an FID detector and a 'J&W Scientific' (Agilent Technologies UK Limited, UK) column with HP-1 stationary phase (30 m × 0.32 mm × 0.25 μm) was used. Gaseous samples of 25 μl were injected into the GC and the temperature program run at 70°C for 3 min and then increased to 80°C at a rate of 5°C min^{-1}. Biomedium *m*-xylene concentration was determined by the concentration of the pollutant in the gaseous phase, utilizing the air-biomedium partition coefficient for *m*-xylene at 30°C, which was determined experimentally as described below. The coefficient of variation for five samples was 4.6% at a concentration level of 0.07 mM *m*-xylene.

Succinate concentration was determined using high-pressure liquid chromatography (HPLC). The analysis was

performed using a Shimadzu liquid chromatograph LC-10AT (Shimadzu, UK) equipped with a SIl-10AD Shimadzu auto injector, a RID-10A Shimadzu refractive index detector and a CTO-10AC column oven. Samples were eluted with distilled water at a flow rate of 0.4 ml min^{-1} from an Aminex HPX-87H (Bio-Rad Laboratories, UK) ion-exclusion organic acid analysis column (300 × 7.8 mm inside diameter) at 55°C. Biomedium samples were centrifuged for 4 min at 11000 r.p.m. and the supernatant solution was filtered through 0.2 μm filters to remove any remaining solids. Fifty microlitres of the filtered sample was injected into the HPLC. The concentration of succinate was calculated interpolating from a previously established succinate calibration curve. The coefficient of variation for three samples was 0.1% at a concentration level of 4.38 mM succinate.

Biomass concentration was determined by absorbance at 600 nm on a UV-2101PC scanning spectrophotometer (Shimadzu, UK) interpolating from a previously established dry weight calibration curve. The coefficient of variation for five samples was 4.2% at a concentration level of 583 (mg biomass) l^{-1}.

Partition coefficient determination

The air-biomedium partition coefficient for *m*-xylene was determined at 30°C. Conical flasks (2.35 l) were filled with 400 ml each of M9. A known mass of *m*-xylene was injected into the flasks, which were stirred with a magnetic stirrer at 30°C. The headspace *m*-xylene concentration was measured by GC analysis at constant time intervals, until equilibrium was established between the phases. The *m*-xylene partition coefficient ($P_{m\text{-}x}$) was determined using the *m*-xylene concentrations in the biomedium ($C_{L,m\text{-}x}$) and in the gas phase ($C_{G,m\text{-}x}$) as follows:

$$P_{m-x} = \frac{C_{L,m-x}}{C_{G,m-x}} \tag{5}$$

Isolation of total RNA, cDNA synthesis and quantitative real-time PCR

Quantitative real-time PCR (Q-PCR) was performed to determine the expression of *xylR*, *xylS* and *rpoN* genes during the course of the experiments. Some 4.5 ml of biomedium samples was centrifuged for 4 min at 11 000 r.p.m. and the supernatant solution was removed. The cell pellet was quenched in liquid N_2 for 1 min and was stored at –80°C. Total RNA was isolated from quenched cells using NucleoSpin RNA II (Fisher Scientific, UK) following the instructions in the manual and was eluted with 60 μl RNase-free water. After the extraction, total RNA was used immediately for cDNA synthesis. cDNA was synthesized using iScript Select cDNA Synthesis Kit (Bio-Rad Laboratories, UK) using random priming. Q-PCR assays were performed on a Rotor-Gene 6000 (Qiagen, UK), using iQ™ SYBR Green Supermix (Bio-Rad Laboratories, UK). For each reaction, 2 μl of cDNA (10 ng μl^{-1}) was mixed with 24 μl of the PCR solution, which contained 12.5 μl 1× iQ SYBR Green Supermix, 0.25 μl of forward primer (0.2 μM) and 0.25 μl of reverse primer (0.2 μM) (Invitrogen, UK) and 11 μl of sterile water. The primer sequences used are displayed in Table 3. PCR reaction was carried out according to the following protocol: initial denaturation at 95°C (3 min) followed by 50 cycles of 95°C (20 s), 60°C (30 s) and 72°C (30 s). A melting curve was generated for each reaction in order to ensure the specificity of each PCR product. Threshold cycle values (C_T) were calculated with the use of Rotor-Gene 6000 series software 1.7 (Qiagen, UK). The reference gene was *rpoN* and was used to normalize the C_T values of *xylR* and *xylS* (Eqs 6–7). A random sample, where both target genes were expressed, was used as the calibrator. Eqs 8–9 were used to normalize the C_T values of *xylR* and *xylS* for the calibrator. $\Delta\Delta C_T$ values of the target genes were determined by subtracting the calibrator ΔC_T value from ΔC_T value of each sample. The normalized levels of *xylR* and *xylS* mRNA expressions (NE_{xylR}, NE_{xylS}) were calculated using Eqs 10–11. Each Q-PCR reaction was performed in duplicate. The coefficient of variation for three samples was 2.8% at a cDNA mass level of 10 ng used for each reaction.

Table 3. Primers used in Q-PCR.

Primer	Description
5 *xyl*R 907 RT	5′-AACTGTTTGGTGTCGATAAGG-3′
3 *xyl*R 1009 RT	3′-ATCACCTCATCAAGAAAGATGG-5′
5 *xyl*S 210 RT	5′-GGATTAGAGACCTGTTATCATCTG-3′
3 *xyl*S 318 RT	3′-GATTGAGCAGCAATAGTTCG-5′
5 *rpo*N 1067 RT	5′-TAACGAAACCCTGATGAAGG-3′
3 *rpo*N 1169 RT	3′-AATGTCATGCAGTACCAACG-5′

$$\Delta C_{T,xylR} = C_{T,xylR} - C_{T,rpoN} \tag{6}$$

$$\Delta C_{T,xylS} = C_{T,xylS} - C_{T,rpoN} \tag{7}$$

$$\Delta\Delta C_{T,xylR} = \Delta C_{T,xylR}(\text{sample}) - \Delta C_{T,xylR}(\text{calibrator}) \tag{8}$$

$$\Delta\Delta C_{T,xylS} = \Delta C_{T,xylS}(\text{sample}) - \Delta C_{T,xylS}(\text{calibrator}) \tag{9}$$

$$NE_{xylR} = 2^{-\Delta\Delta C_{T,xylR}} \tag{10}$$

$$NE_{xylS} = 2^{-\Delta\Delta C_{T,xylS}} \tag{11}$$

Statistical analysis

SigmaStat (Systat Software UK, UK, version 3.5) was used for one-way analysis of variance (ANOVA) in order to elucidate the effect of time for the relative activity of *Pr* and *Ps* promoters. The criterion for the implementation of the ANOVA tests was the normality assumption (Maxwell and Delaney, 2003). The level of significance was accepted at $P < 0.05$. SigmaPlot (Systat, version 8.0) was used for graphical representation of the data.

Parameter estimation in gPROMS

All parameter estimation experiments and model simulations were carried out on an Intel Core™2 Duo (E4600-2.4, 2.39) personal computer with 3.24 GB of RAM memory, and all model simulations and parameter estimation experiments were implemented in the advanced process modelling environment gPROMS. gPROMS is an equation-oriented modelling system used for building, validating and executing first-principles models within a flowsheeting framework.

Parameter estimation in gPROMS is based on the maximum likelihood formulation, which provides simultaneous estimation of parameters in both the physical model of the process as well as the variance model of the measuring instruments. gPROMS attempts to determine values for the uncertain physical and variance model parameters, θ, that maximize the probability that the mathematical model will predict the measurement values obtained from the experiments. Assuming independent, normally distributed measurement errors, ε_{ijk}, with zero means and standard deviations, σ_{ijk}, this maximum likelihood goal can be captured through the following objective function:

$$\Phi = \frac{N}{2}\ln(2\pi) + \frac{1}{2}\min_{\theta}\left\{\sum_{i=1}^{NE}\sum_{j=1}^{NVi}\sum_{k=1}^{NMij}\left[\ln(\sigma_{ihk}^2) + \frac{(\bar{z}_{ijk} - z_{ijk})^2}{\sigma_{ihk}^2}\right]\right\} \quad (12)$$

where N stands for total number of measurements taken during all the experiments, θ is the set of model parameters to be estimated, NE is the number of experiments performed, NV_i is the number of variables measured in the ith experiment and NM_{ij} is the number of measurements of the jth variable in the ith experiment. The variance of the kth measurement of variable j in experiment i is denoted as σ^2_{ijk}, while z_{ijk} is the kth measured value of variable j in experiment i and z_{ijk} is the kth (model-)predicted value of variable j in experiment i. The above formulation can be reduced to a recursive least squares parameter estimation if no variance model for the sensor is selected.

Acknowledgements

This work was supported by the European Union with the following projects: a) PROBACTYS (FP6 – NEST-PATHFINDER EU call on Synthetic Biology, Project Number 029104), b) PSYSMO (BMBF – ERA-NET program on the Systems Biology of Microorganisms, Project Number 0313980) and c) TARPOL (FP7 EU – KBBE Coordination Action for SynBio in Environmental Sciences).

References

Alon, U. (2006) *An Introduction to Systems Biology: Design Principles of Biological Circuits*. Boca Raton, FL, USA: CRC Press.

Aranda-Olmedo, I., Marin, P., Ramos, J.L., and Marques, S. (2006) Role of the *ptsN* gene product in catabolite repression of the *Pseudomonas putida* TOL toluene degradation pathway in chemostat cultures. *Appl Environ Microbiol* **72:** 7418–7421.

Ballerstedt, H., Volkers, R.J.M., Mars, A.E., Hallsworth, J.E., Santos, V.A.M., Puchalka, J., *et al*. (2007) Genomotyping of *Pseudomonas putida* strains using *P. putida* KT2440-based high-density DNA microarrays: implications for transcriptomics studies. *Appl Microbiol Biotechnol* **75:** 1133–1142.

Becskei, A., and Serrano, L. (2000) Engineering stability in gene networks by autoregulation. *Nature* **405:** 590–593.

Bertoni, G., Marques, S., and de Lorenzo, V. (1998) Activation of the toluene-responsive regulator XylR causes a transcriptional switch between σ^{54} and σ^{70} promoters at the divergent *Pr/Ps* region of the TOL plasmid. *Mol Microbiol* **27:** 651–659.

Camas, F.M., Blazquez, J., and Poyatos, J.F. (2006) Autogenous and nonautogenous control of response in a genetic network. *Proc Natl Acad Sci USA* **103:** 12718–12723.

Cases, I., de Lorenzo, V., and Perez-Martin, J. (1996) Involvement of σ^{54} in exponential silencing of the *Pseudomonas putida* TOL plasmid *Pu* promoter. *Mol Microbiol* **19:** 7–17.

De Jong, H. (2002) Modeling and simulation of genetic regulatory systems: a literature review. *J Comput Biol* **9:** 67–103.

Duetz, W.A., Marques, S., de Jong, C., Ramos, J.L., and van Andel, J.G. (1994) Inducibility of the TOL catabolic pathway in *Pseudomonas putida* (pWW0) growing on succinate in continuous culture: evidence of carbon catabolite repression control. *J Bacteriol* **176:** 2354–2361.

Gonzalez-Perez, M.-M., Ramos, J.L., and Marques, S. (2004) Cellular XylS levels are a function of transcription of *xylS* from two independent promoters and the differential efficiency of translation of the two mRNAs. *J Bacteriol* **186:** 1898–1901.

Greated, A., Lambertsen, L., Williams, P.A., and Thomas, C.M. (2002) Complete sequence of the IncP-9 TOL plasmid pWW0 from *Pseudomonas putida*. *Environ Microbiol* **4:** 856–871.

Hasty, J., McMillen, D., and Collins, J.J. (2002) Engineered gene circuits. *Nature* **420:** 224–230.

Hatzimanikatis, V., and Lee, K.H. (1999) Dynamical analysis of gene networks requires both mRNA and protein expression information. *Metab Eng* **1:** 275–281.

Holtel, A., Marques, S., Mohler, I., Jakubzik, U., and Timmis, K.N. (1994) Carbon source-dependent inhibition of *xyl* operon expression of the *Pseudomonas putida* TOL plasmid. *J Bacteriol* **176:** 1773–1776.

Holtel, A., Timmis, K.N., and Ramos, J.L. (1992) Upstream binding sequences of the XylR activator protein and integration host factor in the *xylS* gene promoter region of the *Pseudomonas* TOL plasmid. *Nucleic Acids Res* **20:** 1755–1762.

Holtel, A., Goldenberg, D., Giladi, H., Oppenheim, A.B., and Timmis, K.N. (1995) Involvement of IHF protein in expression of the Ps promoter of the *Pseudomonas putida* TOL plasmid. *J Bacteriol* **177:** 3312–3315.

Hooshangi, S., Thiberge, S., and Weiss, R. (2005) Ultrasensitivity and noise propagation in a synthetic transcriptional cascade. *Proc Natl Acad Sci USA* **102:** 3581–3586.

de Lorenzo, V., Herrero, M., Metzke, M., and Timmis, K.N. (1991) An upstream XylR- and IHF-induced nucleoprotein complex regulates the σ^{54}-dependent *Pu* promoter of TOL plasmid. *EMBO J* **10:** 1159–1167.

Ishihama, A. (1999) Modulation of the nucleoid, the transcription apparatus, and the translation machinery in bacteria for stationary phase survival. *Genes Cells* **4:** 135–143.

Ishihama, A. (2000) Functional modulation of *Escherichia coli* RNA polymerase. *Annu Rev Microbiol* **54:** 499–518.

Jishage, M., Iwata, A., Ueda, S., and Ishihama, A. (1996) Regulation of RNA polymerase sigma subunit synthesis in *Escherichia coli*: intracellular levels of four species of sigma subunit under various growth conditions. *J Bacteriol* **178:** 5447–5451.

Jurado, P., Fernandez, L.A., and de Lorenzo, V. (2003) Sigma 54 levels and physiological control of the *Pseudomonas putida Pu* promoter. *J Bacteriol* **185:** 3379–3383.

Kiparissides, A., Kucherenko, S.S., Mantalaris, A., and Pistikopoulos, E.N. (2009) Global sensitivity analysis challenges in biological systems modeling. *Ind Eng Chem Res* **48:** 7168–7180.

Kitano, H. (2001) Looking beyond the details: a rise in system-oriented approaches in genetics and molecular biology. *Curr Genet* **41:** 1–10.

Kontoravdi, C., Asprey, S.P., Pistikopoulos, E.N., and Mantalaris, A. (2005) Application of global sensitivity analysis to determine goals for design of experiments: an example study on antibody-producing cell cultures. *Biotechnol Prog* **21:** 1128–1135.

McAdams, H.H., and Shapiro, L. (1995) Circuit simulation of genetic networks. *Science* **269:** 650–656.

Marques, S., Gallegos, M.T., Manzanera, M., Holtel, A., Timmis, K.N., and Ramos, J.L. (1998) Activation and repression of transcription at the double tandem divergent promoters for the *xylR* and *xylS* genes of the TOL plasmid of *Pseudomonas putida*. *J Bacteriol* **180:** 2889–2894.

Maxwell, S., and Delaney, H. (2003) *Designing Experiments and Analysing Data: A Model Comparison Perspective*. London, UK: Lawrence Erlbaum Associates.

Merrick, M.J. (1993) In a class of its own – the RNA polymerase sigma factor σ^{54} (σ^{N}). *Mol Microbiol* **10:** 903–909.

Nogales, J., Palsson, B.O., and Thiele, I. (2008) A genome-scale metabolic reconstruction of *Pseudomonas putida* KT2440: *i*JN746 as a cell factory. *BMC Syst Biol* **2:** 79.

Perez-Martin, J., and de Lorenzo, V. (1995) The σ^{54}-dependent promoter *Ps* of the TOL plasmid of *Pseudomonas putida* requires HU for transcriptional activation in vivo by XylR. *J Bacteriol* **177:** 3758–3763.

Pieper, D.H., Santos, V.A.P., and Golyshin, P.N. (2004) Genomic and mechanistic insights into the biodegradation of organic pollutants. *Curr Opin Biotechnol* **15:** 215–224.

Process Systems Enterprise (1997–2010) *gPROMS* [WWW document]. URL http://www.psenterprise.com/gproms.

Puchalka, J., Oberhardt, M.A., Godinho, M., Bielecka, A., Regenhardt, D., Timmis, K.N., *et al*. (2008) Genome-scale reconstruction and analysis of the *Pseudomonas putida* KT2440 metabolic network facilitates applications in biotechnology. *PLoS Comput Biol* **4:** e1000210.

Radivoyevitch, T. (2009) Mass action models versus the Hill model: an analysis of tetrameric human thymidine kinase I positive cooperation. *Biol Direct* **4:** 49.

Ramos, J.L., Mermod, N., and Timmis, K.N. (1987) Regulatory circuits controlling transcription of TOL plasmid operon encoding *meta*-cleavage pathway for degradation of alkylbenzoates by *Pseudomonas*. *Mol Microbiol* **1:** 293–300.

Ramos, J.L., Marques, S., and Timmis, K.N. (1997) Transcriptional control of the *Pseudomonas* TOL plasmid catabolic operons is achieved through an interplay of host factors and plasmid-encoded regulators. *Annu Rev Microbiol* **51:** 341–372.

Rosenfeld, N., Young, J.W., Alon, U., Swain, P.S., and Elowitz, M.B. (2005) Gene regulation at the single-cell level. *Science* **307:** 1962–1965.

Sambrook, J., Fritsch, E.F., and Maniatis, E. (1989) *Molecular Cloning: A Laboratory Manual*. New York, NY, USA: Cold Spring Harbour Press.

Shen-Orr, S.S., Milo, R., Mangan, S., and Alon, U. (2002) Network motifs in the transcriptional regulation network of *Escherichia coli*. *Nat Genet* **31:** 64–68.

Sidoli, F.R., Mantalaris, A., and Asprey, S.P. (2004) Modelling of mammalian cells and cell culture processes. *Cytotechnology* **44:** 27–46.

Timmis, K.N. (2002) *Pseudomonas putida*: a cosmopolitan opportunist *par* excellence. *Environ Microbiol* **4:** 779–781.

Weiss, R. (2001) Cellular computation and communications using engineered genetic regulatory networks. PhD Thesis. Cambridge, MA, USA: MIT.

Weiss, R., Basu, S., Hooshangi, S., Kalmbach, A., Karig, D., Mehreja, R., and Netravali, I. (2003) Genetic circuit building blocks for cellular computation, communications, and signal processing. *Nat Comput* **2:** 47–84.

Wierckx, N.J.P., Ballerstedt, H., de Bont, J.A.M., de Winde, J.H., Ruijssenaars, H.J., and Wery, J. (2008) Transcriptome analysis of a phenol-producing *Pseudomonas putida* S12 construct: genetic and physiological basis for improved production. *J Bacteriol* **190:** 2822–2830.

Zaslaver, A., Mayo, A.E., Rosenberg, R., Bashkin, P., Sberro, H., Tsalyuk, M., *et al*. (2004) Just-in-time transcription program in metabolic pathways. *Nat Genet* **36:** 486–491.

Nomenclature

$C_{L,m\text{-}x}$	*m*-Xylene concentration in the biomedium [mM]
$C_{G,m\text{-}x}$	*m*-Xylene concentration in the gas phase [mM]
$K_{Pr,XylRi}$	$XylR_i$ translation coefficient [–]
$K_{SUC,Pr}$	Inhibition constant of succinate on *Pr* promoter activity [mM^{-2}]
$K_{SUC,Ps}$	Inhibition constant of succinate on *Ps* promoter activity [mM]
K_{XylRa}	Repression coefficient of *Pr* promoter (due to $XylR_a$ binding) [mM]
$K_{XylRa,Ps}$	Activation coefficient of *Ps* promoter [mM]
K_{XylRi}	Repression coefficient of *Pr* promoter (due to $XylR_i$ binding) [mM]
$n_{Pr,a}$	Hill coefficient of *Pr* promoter (due to $XylR_a$ binding) [–]
$n_{Pr,i}$	Hill coefficient of *Pr* promoter (due to $XylR_i$ binding) [–]
$n_{Ps,a}$	Hill coefficient of *Ps* promoter (due to $XylR_a$ binding) [–]
$P_{m\text{-}x}$	Air-biomedium partition coefficient for *m*-xylene [–]
Pr_{TC}	*Pr* promoter relative activity [–]
Ps_{TC}	*Ps* promoter relative activity [–]
$r_{R,XylR}$	$XylR_a$ dissociation constant [$mM^{-1}\ h^{-1}$]
r_{XylR}	$XylR_i$ oligomerization constant [$mM^{-1}\ h^{-1}$]
Suc	Succinate concentration [mM]
t	Time [h]
Xyl	Total *m*-xylene concentration [mM]
Xyl_{INI}	Total *m*-xylene initial concentration [mM]

$XylR_a$ $XylR_a$ protein concentration [mM]
$XylR_i$ $XylR_i$ protein concentration [mM]

Greek letters

α_{Pr} *Pr* promoter deactivation rate [h^{-1}]
α_{Ps} *Ps* promoter deactivation rate [h^{-1}]
α_{XylRi} $XylR_i$ degradation/dilution rate [h^{-1}]
α_{XylRa} $XylR_a$ degradation/dilution rate [h^{-1}]
β_0 Basal expression level of *Ps* promoter [h^{-1}]
β_{Pr} Maximal expression level of *Pr* promoter [h^{-1}]
β_{Ps} Maximal expression level of *Ps* promoter [h^{-1}]
β_{XylRi} Maximal $XylR_i$ translation rate based on *Pr* activity [mM h^{-1}]